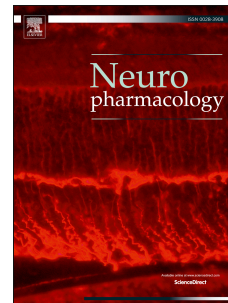


Accepted Manuscript

Riluzole attenuates the efficacy of glutamatergic transmission by interfering with the size of the readily releasable neurotransmitter pool

Vesna Lazarevic, Yunting Yang, Daniela Ivanova, Anna Fejtova, Per Svenningsson



PII: S0028-3908(18)30660-9

DOI: [10.1016/j.neuropharm.2018.09.021](https://doi.org/10.1016/j.neuropharm.2018.09.021)

Reference: NP 7346

To appear in: *Neuropharmacology*

Received Date: 23 April 2018

Revised Date: 11 August 2018

Accepted Date: 12 September 2018

Please cite this article as: Lazarevic, V., Yang, Y., Ivanova, D., Fejtova, A., Svenningsson, P., Riluzole attenuates the efficacy of glutamatergic transmission by interfering with the size of the readily releasable neurotransmitter pool, *Neuropharmacology* (2018), doi: <https://doi.org/10.1016/j.neuropharm.2018.09.021>.

This is a PDF file of an unedited manuscript that has been accepted for publication. As a service to our customers we are providing this early version of the manuscript. The manuscript will undergo copyediting, typesetting, and review of the resulting proof before it is published in its final form. Please note that during the production process errors may be discovered which could affect the content, and all legal disclaimers that apply to the journal pertain.

Riluzole attenuates the efficacy of glutamatergic transmission by interfering with the size of the readily releasable neurotransmitter pool

Vesna Lazarevic, Ph.D.^{1*}, Yunting Yang, Ph.D.¹, Daniela Ivanova, Ph.D.^{2#}, Anna Fejtova, Ph.D.^{2,3}, Per Svenningsson, Ph.D.¹

¹ Translational Neuropharmacology, Department of Clinical Neuroscience, Center for Molecular Medicine, Karolinska Institute, Stockholm, Sweden

² RG Presynaptic Plasticity, Leibniz Institute for Neurobiology, Magdeburg, Germany

³ Molecular Psychiatry, Department of Psychiatry and Psychotherapy, University Hospital, Friedrich-Alexander-University Erlangen-Nuremberg, Erlangen, Germany

[#] Present address: Centre for Integrative Physiology, Hugh Robson Building, George Square, University of Edinburgh, Edinburgh, Scotland, UK

***Corresponding Author:**

Vesna Lazarevic
Department of Clinical Neuroscience
Neuro Svenningsson, CMM L8:01,
Karolinska Universitetssjukhuset
171 76 Stockholm, Sweden
Tel. +46-8-51774614
Fax. +46-8-51774614
E-mail: vesna.lazarevic@ki.se

Abstract

Riluzole is a potent neuroprotective agent which primarily inhibits excitatory neurotransmission interfering with presynaptic release, uptake and postsynaptic actions of glutamate by mechanisms that are not well understood. Riluzole and related prodrugs with improved blood brain barrier penetrance, are shown to be effective for the treatment of amyotrophic lateral sclerosis, ataxias, epilepsy and mood disorders. Our study was undertaken to decipher molecular and subcellular mechanisms of riluzole's ant glutamatergic effect, particularly focusing on presynaptic active zone structure and function. Applying multifarious live cell imaging techniques and amperometric glutamate recordings, we measured the impact of riluzole on presynaptic activity, synaptic vesicle recycling and glutamate release. Our *in vitro* and *in vivo* data revealed a unique mechanism whereby riluzole reduces the efficacy of glutamatergic transmission by selectively lowering the size of the readily releasable pool. This effect was correlated with the inhibition of protein kinase C-dependent Munc18-1 phosphorylation which is known to interfere with neurotransmitter release.

Keywords: riluzole, glutamate, presynaptic activity, synaptic vesicle recycling, PKC

1. Introduction

As the principal excitatory neurotransmitter in the central nervous system (CNS), glutamate plays a crucial role in many brain functions including neuronal differentiation, migration, synaptic transmission, synaptic plasticity and learning and memory processes. However, an excess of glutamate is the most common pathogenic feature of many neurological and neurodegenerative disorders, ultimately leading to synaptic and neuronal dysfunctions and cell death. Therefore, the level of glutamate has to be strictly maintained within the nervous system and agents that modulate its release and/or re-uptake have a great potential as therapeutics.

Riluzole (2-amino-6-trifluoromethoxy benzothiazole) is an antiglutamatergic neuroprotective drug approved for the treatment of amyotrophic lateral sclerosis (Bruijn et al., 2004). ALS is a neurodegenerative motor neuron disease affecting not only the peripheral but also the central nervous system and it has been shown that riluzole increases survival time in ALS. Initially, riluzole was developed as an antiepileptic agent with activity against both limbic and absence seizures (Borowicz et al., 2004; Kim et al., 2007a). The most common cause of epilepsy is an increased ratio between excitatory (E) and inhibitory (I) neurotransmission and by targeting glutamate release riluzole may contribute to the recovery of E/I balance on both synaptic and circuit levels. Recent studies showed that riluzole treatment may slow down progression of ataxias (Romano et al., 2015) and age-related cognitive decline (Hunsberger et al., 2015; Pereira et al., 2014) suggesting also a potential use of riluzole as a therapeutic agent for AD. In addition, riluzole has been extensively studied in the context of treatment-resistant depression and other mood disorders in which excess of glutamate is a part of the pathological mechanism (Grant et al., 2010; Lener et al., 2017; Salardini et al., 2016; Sanacora et al., 2007). Indeed, the hypothesis that mood/anxiety disorders are accompanied by a reduced availability of monoamines has been expanded to the “neuroplasticity hypothesis” that also involves the role of glutamate and excitatory transmission in mediating the complex emotional and cognitive changes associated with depression (Duman and Aghajanian, 2012; Sanacora et al., 2012). Therefore, antiglutamatergic agents, including ketamine, and riluzole, have gained increased attention in the fields of neuropsychopharmacology and biological psychiatry (Grant et al., 2010). Some of the recent clinical data, however, reported limited efficacy of riluzole as a monotherapy in this

regard, but still suggesting its potential as adjunctive therapy in the treatment of acute bipolar depression (Mathew et al., 2017; Park et al., 2017).

Several mechanisms have been implicated in mediating the antiglutamatergic actions of riluzole, but the detailed molecular aspects are not yet completely understood. A major mode of action is the reduction of glutamate release from presynaptic nerve terminals most likely by blocking voltage gated sodium channels (Urbani and Belluzzi, 2000) and/or through a reduction in the calcium influx mediated by P/Q-type calcium channels (Kim et al., 2007a). There are also evidences that riluzole modulates receptor-mediated effects, mainly at the postsynaptic site (Umemiya and Berger, 1995) (Centonze et al., 1998) (Zona et al., 2002) (Pereira et al., 2014). Additionally, riluzole increases glial glutamate reuptake (Frizzo et al., 2004; Fumagalli et al., 2008) which further contributes to its protective and antidepressant-like property.

Using state-of-the art methodological approaches, we investigated the impact of riluzole on presynaptic release probability, synaptic vesicle (SV) pools and the underlying molecular mechanisms. Our *in vitro* and *in vivo* data revealed a unique mechanism whereby riluzole reduces the efficacy of glutamatergic transmission by selectively lowering the size of the readily releasable pool (RRP), namely by interfering with the docking step of SV cycling. At the biochemical level, riluzole decreased protein kinase C (PKC) dependent Munc18-1 phosphorylation, which is known to interfere with neurotransmitter release.

2. Materials and methods

2.1. Animals

Time pregnant Wistar rats used for preparation of primary cortical cells and male C57BL/6J mice used for Fast Analytic Sensing Technology (FAST) experiments were obtained from Charles River (Sulzfeld, Germany). Animal procedures were performed in agreement with the European Council Directive (86/609/EEC) and approved by the local Animal Ethics Committee (Stockholms Norra Djurförsöksetiska Nämnd, approval number N24/12, N269/13). All efforts were made to minimize suffering and the number of animals used.

2.2. Drugs and toxins

Riluzole hydrochloride (100 μ M), D-AP5 (50 μ M), CNQX (10 μ M), MG132 (10 μ M), Phorbol 12, 13-dibutyrate (PMA, 2nM), Bryostatins 1 (0.27 nM), Calphostin C (1 μ M), Ro 31-8220 (3.3 μ M) were purchased from Tocris (Bristol, United Kingdom).

2.3. Antibodies

Primary polyclonal antibodies from rabbit were as follows: Bassoon (ICC 1:1000, Synaptic Systems); Munc13-1 (WB; ICC 1:1000, Synaptic Systems); Rim1/2 (WB; ICC 1:1000, Synaptic Systems); Synaptophysin (WB 1:1000, Sigma); Synaptotagmin 1/2 cytoplasmic domain (WB; ICC 1:1000, Synaptic Systems); VGAT (ICC 1:500, Synaptic Systems); VGLUT1 (ICC 1:500, Synaptic Systems); Munc18-1 phospho S313 (WB, ICC 1:500, Abcam); Homer 1 (WB; ICC 1:1000, Synaptic Systems), GluR1 (ICC 1:1000, Upstate). Primary monoclonal antibodies from mouse: Synaptotagmin 1 luminal domain fluorescence labeled with Oyster[®] 550 (ICC 1:250 Synaptic Systems); Synaptotagmin 1 luminal domain fluorescence-labeled with CypHer5E (ICC 1:100 Synaptic Systems); GluA/AMPA fluorescence labeled with Oyster[®] 550 (ICC 1:250 Synaptic Systems); Munc18-1 (WB; ICC 1:1000, Synaptic Systems); PSD95 (WB; ICC 1:1000, Synaptic Systems); SNAP25 (WB; ICC 1:1000, Synaptic Systems); beta III Tubulin (WB 1:2000, Sigma). Primary polyclonal antibodies from guinea pig: Synaptophysin 1 (ICC 1:500 Synaptic Systems). Fluorescently labeled secondary antibodies used for ICC were purchased from Thermo Scientific and used in dilution 1:1000: anti-rabbit Alexa Fluor[®] 488 conjugate; anti-mouse Alexa Fluor[®] 568 conjugate; anti-guinea pig Alexa Fluor[®] 647 conjugate. Fluorescently labeled

secondary antibodies used for WB were obtained from Li-COR: anti-rabbit IRDye 800CW (1:30.000) and anti-mouse IRDye 680RD (1:30.000).

2.4. Primary cortical neurons

Primary cortical neurons were prepared as described previously (Lazarevic et al., 2011). Neurons were plated either on poly-D-lysine-coated glass coverslips (round 12mm, A. Hartenstein GmbH) for immunocytochemistry (50.000 cells/coverslip) or on six well plates for biochemical analysis (300.000 cells/well). For Synaptotagmin-1-cypHer imaging cortical neurons were plated on 18 mm round glass coverslip at density of 100.000 cells/coverslip. Cells were kept in a humidified incubator with 5% CO₂ for up to 3 weeks.

2.5. Immunocytochemistry and functional imaging

Cells were fixed with 4% paraformaldehyde for 3 min and blocked/permeabilized with phosphate buffer solution (PBS) containing 10% FBS, 0.1% glycine and 0.3% TritonX-100 for 30min at room temperature. Primary antibodies diluted in 3% fetal bovine serum in PBS were applied overnight at 4°C and after three washing steps with PBS, coverslips were incubated with secondary antibodies for one hour at room temperature. Mowiol (Calbiochem) was used as a mounting medium to embed coverslips onto microscopic slides. Slides were kept at 4°C until analysis. Functional imaging using Anti-Synaptotagmin1 luminal domain antibody labeled with Oyster® 550 (Syt1-L ab uptake) and Anti-GluA/AMPA fluorescence-labeled with Oyster® 550 was carried out as previously described (Lazarevic et al., 2011). Both control and treated cells were briefly washed with freshly prepared Tyrode's buffer and incubated with fluorescently-labeled syt1-L or GluA/AMPA antibody diluted in the same buffer for 20 min at 37°C. To assess the size of RRP, syt1-L ab uptake was done in hypertonic solution containing 500 mM sucrose. Afterwards, cells were fixed and processed for immunocytochemistry as described above. For each condition, 2 coverlips were processed in parallel.

2.6. Synaptotagmin-1-cypHer imaging

To label all active synapses, 16-20 days old primary cortical neurons were incubated for 3 hours at 37°C in a buffer containing 120 mM NaCl, 5 mM KCl, 2 mM MgCl₂, 2 mM CaCl₂, 10 mM glucose, and 18 mM NaHCO₃, pH 7.4 with CypHerTM5E anti-synaptotagmin1 antibody (1:100).

Thereafter, the coverslips were placed in an imaging chamber, supplied with a pair of platinum wire electrodes, 10 mm apart, for electrical stimulation and live imaging was performed at 26°C in presence of 1µM of Bafilomicyn A1 (Calbiochem) on an inverted microscope (Observer. D1; Zeiss) equipped with an EMCCD camera (Evolve 512; Photometrics) controlled by VisiView (Visitron Systems GmbH) software, using 63x objective and Cy5 ET filter set (exciter 620/60, emitter 700/75, dichroic 660 LP) (Chroma Technology Corp.). A stream of images was acquired at 10Hz. The action potentials were evoked by delivering 1ms constant voltage pulses at 20Hz using S48 stimulator (GRASS Technologies). The readily releasable pool (RRP) was released by stimulation with 40AP. To reveal the size of the recycling pool (RP), 200AP were delivered, following a break of 2 min after the end of the first train of stimuli. The relative sizes of the RRP and the RP were determined as fractions of the total Syt1-L-CypHer labeling. The synaptic puncta responding to stimulation were identified by subtracting the average of 10 frames directly after the onset of stimulation from the average of the first 10 frames of the baseline (before stimulation). The mean IF intensities were measured in ROIs with a radius of 1.87 µm, centered over each responding synapse using a custom-made macro in ImageJ (NIH, <http://rsb.info.nih.gov/ij/>). The fluorescence traces were corrected for bleaching and a bleaching factor was estimated from the bleaching of the naive puncta on the same image.

2.7. siRNA transfections

SMARTpool Accell Stxbp1 siRNA was purchased from Dharmacon. As a control the cells were treated with Accell Non-targeting Pool siRNA. The procedure was essentially done according to manufacturer's protocol. Briefly, primary cortical neurons were transfected either with Stxbp1 (Munc18-1) siRNA pool or with non-targeting pool siRNA for 96h. 90 min before proceeding with western blot or functional imaging cells were treated with control solution or riluzole.

2.8. Immunoblotting

For all immunoblot analysis the whole cell lysate was used. Cortical cells were maintained for 3 weeks *in vitro*, treated as indicated and washed briefly with ice cold washing buffer (10mM Tris, 300mM sucrose pH 7.4). Thereafter, cells were lysed in a buffer containing 10mM Tris-HCl (pH 7.4), 150mM NaCl, 2% SDS, 1% Deoxycholate, 1% TritonX-100. Prior to use the buffer was supplemented with protease and phosphatase inhibitor cocktail (Halt, Thermo Fisher Scientific).

Lysates were centrifuged for 10min at 2000 x g to eliminate cell debris. Protein concentration was determined by the colorimetric BCA Protein Assay (Pierce) and equal protein amounts were loaded onto a polyacrylamide gel. Proteins were separated using one-dimensional sodium dodecyl sulfate polyacrylamide gel electrophoresis (SDS-PAGE) under fully denaturing and reducing conditions and electrotransferred to Millipore Immobilon-FL transfer membranes. Primary antibodies diluted in TBS-T containing 5 % of BSA and 0.025% of sodium azide were applied over-night. After three washing steps with TBS-T for 10 minutes each time, the membranes were submerged in fluorescently-labeled secondary antibodies diluted in TBS-T containing 5 % of BSA and 0.01% of SDS and incubated for 1 hour at room temperature. After four washing steps in TBS-T and two washings in TBS, membranes were scanned in the appropriate channels (700 or 800 nm) using Odyssey CLx Infra Red Imaging system from LI-COR Biosciences (Lincoln, Nebraska USA). Quantification of the signals was done using software Image Studio 3.1. From obtained intensity for each band the background subtraction was made and all the values were normalized to beta-III-Tubulin referred as a loading control.

2.9. Biotinylation Assay of AMPA Receptor-Surface Expression

Three weeks old control and treated primary cortical neurons were placed on ice and rinsed with ice cold PBS. Cells were incubated for 20 min in PBS containing 1.5 mg/ml of Sulfo-NHS-LC-Biotin (Thermo Fisher Scientific), washed two times with ice cold PBS and lysed in a lysis buffer containing 0.1% SDS, 1% TritonX-100 and phosphatase inhibitors. After a brief centrifugation step (15 min at 2000xg) in order to eliminate aggregates and cell debris, 10% of the total lysate was preserved and used as an input to estimate the total level. The rest of the lysate was added to NeutrAvidin-agarose beads (Thermo Fisher Scientific) and put under mild agitation for 2h at 4°C. Following the incubation, the resin was washed five times with a washing buffer containing 0.1% SDS, 1% TritonX-100 in PBS. After final washing step biotinylated surface proteins were eluted in 70 µl of 2X Laemmli buffer and processed for subsequent western blot analysis.

2.10. In vivo amperometry measurements of glutamate

In vivo recording of glutamate release was performed using an enzyme-based method as previously described (Alvarsson et al., 2015). In brief, mice were anesthetized with isoflurane (Baxter Medical, Kista, Sweden) and placed in a stereotaxic frame fitted with a Cunningham

mouse adapter (Stoelting, Wood Dale, IL, USA). Small craniotomies were performed bilaterally above the regions of interest to expose the brain and an additional hole was made for Ag/AgCl reference electrode. The MEA was then lowered into the region of interest (coordinates: prefrontal cortex AP +1.8, ML \pm 0.3, DV -2.1 (PL) -2.6 (IL)). A potential of +0.7 V was applied against the reference electrode and the Fast Analytic Sensing Technology recording system (FAST-16 MKII, Quanteon LLC, Nicholasville, KY, USA) recorded the amperometric data at a rate of 2 Hz. The signal was allowed to stabilize for at least 20 minutes before local pressure ejections of 130 μ l isotonic potassium chloride (70mM KCl, pH \sim 7.4) with/without 100 μ M Riluzole or 0.2 μ M PMA were made to evoke the endogenous release of glutamate at 1 minute intervals. FAST Analysis 4.1 software (Quanteon) was used for data analysis. The first two pressure ejections were excluded from analysis, and the following 3-5 events were averaged for maximum amplitude of evoked glutamate.

2.11. Image acquisition and analysis

Images were acquired by ZEISS LSM 880 Airyscan confocal laser scanning microscopy equipped with ZEN2.1 software, using Plan-Apochromat 63x/1.4 Oil DIC M27 63x oil objective. For each experiment the same settings were applied to control and treated coverslips and images were taken from at least two different coverslips for each condition to avoid effects given by experimental variance. Quantitative immunofluorescence analyses were performed using ImageJ (NIH, <http://rsb.info.nih.gov/ij/>) and OpenView software (Tsuruel et al., 2006). Following appropriate background subtraction immunoreactive puncta were counted along 20 μ m of the proximal dendrite (<50 μ m distance from the cell body). The synaptic immunofluorescence intensities were assessed in a region of interest (ROI) set by the mask in the channel for Synaptophysin which was used as synaptic marker. The mask (with dimensions about 0.8 \times 0.8 μ m) was created semiautomatically using OpenView software. Images were adjusted for presentation using ImageJ and Photoshop (Adobe Systems).

2.12. Statistics

In all experiments, statistical analyses were done using GraphPad Prism, version 5.04. using two-way ANOVA or Student's t-test. A normal distribution of the data was assessed by D'Agostino-Pearson test. For each experimental setup, data were normalized to the mean of the control group

and expressed as mean \pm SEM. Statistical significance was assessed as * $p < 0.05$; ** $p < 0.01$; *** $p < 0.001$; **** $p < 0.0001$.

3. Results

3.1. Riluzole attenuates the efficacy of presynaptic glutamatergic transmission

The effect of the glutamate modulator, riluzole, on presynaptic activity was evaluated by imaging synaptic vesicle turnover using a fluorophore coupled antibody against the luminal domain of the integral synaptic vesicle protein synaptotagmin-1 (Syt1-L ab uptake). Our data revealed that primary cortical neurons exposed to a short term treatment with riluzole (100 μ M; 90 min) showed significantly reduced network activity driven presynaptic release in comparison to untreated cells and this inhibitory action of the drug was completely reversed 24 hours after washout (two-way ANOVA; riluzole $F_{1,63}=5.07$, $p=0.0279$; washout $F_{1,63}=11.41$, $p=0.0013$) (Fig.1.A,B). Obtained data implied that riluzole does not induce permanent changes in synaptic release, but has rather a modulatory function. When cells were exposed to the lower concentration of the drug (1 μ M and 10 μ M) no significant changes in Syt1-L ab uptake were observed (supplementary fig. S1). Therefore, all further experiments were done using 100 μ M riluzole.

Riluzole's antiglutamatergic efficacy was also evaluated in neurons where presynaptic potentiation and the increased glutamate release was induced by prolonged network activity deprivation. Exposing neurons to NMDA (50 μ M D-AP5) and AMPA (10 μ M CNQX) receptor antagonists for 48h induces a homeostatic presynaptic strengthening indicated as an increase in Syt1-L ab uptake (Lazarevic et al., 2011). As shown in Fig.1.C,D, riluzole application for 90 min completely reversed the inactivity-induced homeostatic presynaptic strengthening revealing a striking property of the drug to reduce recycling of presynaptic SV (two-way ANOVA; D-AP5/CNQX $F_{1,67}=6.44$, $p=0.0135$; riluzole $F_{1,67}=60.95$, $p < 0.0001$).

Quantification of Syt1-L ab uptake in puncta positive for either excitatory (Vesicular Glutamate Transporter, VGLUT1) or inhibitory marker (Vesicular GABA Transporter, VGAT) showed that riluzole selectively reduced the activity only in excitatory, glutamatergic synapses without affecting inhibitory, GABAergic synapses ($t(33)=3.771$, $p=0.0006$ in VGLUT1 positive puncta;

$t(26)=1.535$, $p=0.1369$ in VGAT positive puncta) (Fig.1.E,F). Selective effect on Syt1-L ab uptake in excitatory synapses also suggests that riluzole affects recycling of glutamatergic SVs rather than overall network activity. Moreover, the synaptic level of VGLUT1 which is in charge of glutamate loading into SVs, was significantly downregulated in cells exposed to riluzole ($t(34)=5.081$, $p<0.0001$) (Fig.1.E,G). Interestingly, although the activity of inhibitory synapses was not changed in riluzole challenged neurons, synaptic level of the GABA transporter (VGAT) was increased in comparison to untreated cells ($t(27)=2.596$, $p=0.0151$) (Fig.1.E,G). This may suggest increased GABA load into SV and potentially increased quantal GABA release.

3.2. Riluzole decreases the size of the readily releasable pool

Ex vivo data from purified cerebrocortical synaptosomes showed that riluzole impairs depolarization evoked glutamate release (Wang et al., 2004) implying its influence on recycling vesicle pools. In order to visualize the impact of riluzole on the size of the SV pools and the kinetics of SV exocytosis in living neurons, we monitored the release of synaptotagmin1 using the anti lumenal domain antibody coupled to the pH sensitive fluorophore cypHer5E (Andreae et al., 2012; Hua et al., 2011). CypHer5E fluorescence is quenched upon exposure to the neutral extracellular pH after SV exocytosis. Recycling vesicles were pre-labeled with the Syt1-L-CypHer antibody and SV exocytosis was evoked by field stimulation in the presence of bafilomycin A, a specific inhibitor of vacuolar proton ATPases used to prevent SV re-acidification after exocytosis. Cells were first stimulated at 20Hz with 40AP in order to deplete RRP and subsequently, with a train of 200AP to release the rest of the recycling-competent vesicles (referred as total recycling pool, tRP). As shown in Fig.2.A, riluzole significantly influenced the size of RRP, having no impact on the size of tRP (RRP: $t(10)=3.451$, $p=0.0062$; tRP: $t(10)=0.1695$, $p=0.8688$). The effect of riluzole on RRP was further confirmed by Syt1-L ab uptake assay performed in the presence of hypertonic solution which is routinely used to deplete RRP (Alabi and Tsien, 2012; Rosenmund and Stevens, 1996). This experiment showed a significant reduction of Syt1-L ab uptake in riluzole treated cells upon stimulation with 500 mM sucrose revealing the effect of the drug on size of RRP ($t(36)=6.097$, $p<0.0001$) (Fig.2.B,C). RRP is defined as the pool of synaptic vesicles that are primed and immediately available for release upon neuronal stimulation. Morphologically those vesicles are docked to presynaptic plasma membrane suggesting that riluzole might interfere with the priming/docking step of the SV cycle.

3.3. Riluzole induces pre- and postsynaptic remodeling

Release of glutamate is a tightly controlled process that involves orchestrated action of both presynaptic and postsynaptic compartments. Functional changes in presynaptic efficacy are tightly coupled to molecular remodeling of the proteins involved in neurotransmission (Gundelfinger and Fejtova, 2012) (Lazarevic et al., 2011). Therefore, we investigated if riluzole has an impact on the synaptic and cellular level of selected pre- and postsynaptic proteins. Employing a quantitative immunocytochemical approach, we showed that synaptic level of integral SV proteins, SNARE proteins and presynaptic scaffolds involved in the spatiotemporal organization of the SV cycle were indeed significantly affected by riluzole application. The synaptic amounts of most presynaptic proteins were significantly decreased, with the exception of RIM which showed elevated synaptic abundance (Synaptophysin (Sph) $t(71)=4.231$, $p<0.0001$; SNAP25 $t(49)=3.427$, $p=0.0012$; Synaptotagmin1/2 (Syt1/2) $t(39)=4.934$, $p<0.0001$; Bassoon (Bsn) $t(72)=4.291$, $p<0.0001$; Piccolo (Pclo) $t(45)=2.127$, $p=0.039$; Munc13-1 $t(49)=3.053$, $p=0.0037$; RIM1/2 $t(60)=3.292$, $p=0.0017$; Synapsin (Syn) $t(46)=1.483$, $p=0.1450$) (Fig.3.A,B). Blocking of proteasomes prior riluzole application did not prevent riluzole induced reduction of selected proteins at the level of individual synapses (supplementary fig. S2) and results obtained by quantitative western blotting showed that total cellular level of the above mentioned proteins was not changed upon 90 min of riluzole treatment (supplementary fig. S3). Together, these data indicate that riluzole does not modify expression or degradation but rather the dynamic recruitment of these proteins to the presynaptic boutons.

Changes in the presynaptic release probability significantly influence postsynaptic neuronal glutamate sensitivity, primarily the number and turnover of AMPA receptors (O'Brien et al., 1998). It was previously suggested that riluzole regulates AMPA receptors membrane localization (Du et al., 2007). Using biotinylation assay, we corroborated the previous finding by showing that riluzole induced alterations in presynaptic efficacy led to a compensatory enhancement of the surface GluA1 expression without affecting its total level (Fig.3.C). Likewise, live staining of primary cortical neurons with fluorescence-labeled GluA antibody revealed increased surface GluA immunoreactive puncta in riluzole exposed cells in comparison to untreated controls ($t(43)=4.052$, $p=0.0002$) (Fig.3.D,E). By immunocytochemical validation we further showed that the postsynaptic scaffolding protein PSD95 which promotes surface

recruitment of AMPA receptors (Kim et al., 2007b) was also upregulated in cells treated with riluzole ($t(35)=2.691$, $p=0.0108$) (Fig. 3.F,G). However, under the same condition, synaptic level of other postsynaptic protein, Homer1, was significantly lowered ($t(34)=4.476$, $p<0.0001$) (Fig.3.F,G). As shown in Fig S3, the total expression level of those postsynaptic proteins was not affected by the treatment with riluzole.

Taken together, the obtained data indicate that the antiglutamatergic effect of riluzole is accompanied by molecular remodeling at both pre- and postsynapse that most probably drives the drug-induced changes in neurotransmission. Interestingly, this remodeling is not primarily driven by changes in expression of the synaptic proteins, but rather by changes in their synaptic recruitment.

3.4.Riluzole attenuates SV recycling by inhibiting PKC-dependent Munc18 phosphorylation

Protein kinase C (PKC) is one of the well-known signaling molecules involved in regulation of neurotransmission and dynamics of SV recycling, specifically targeting RRP. Phorbol esters, which directly activate PKC, increase both the size of RRP and the rate at which the pool refills (Stevens and Sullivan, 1998). Previously it was shown that riluzole directly inhibits the activity of PKC in primary cortical neurons (Noh et al., 2000). To explore the possibility that riluzole-mediated synaptic attenuation involves PKC action in our model system, we assessed the presynaptic function in the presence or absence of riluzole in cells where the activity of the kinase was pharmacologically altered. As expected, PMA-mediated activation of PKC increases the rate of release probability which could be completely hindered by the presence of riluzole (two-way ANOVA; PMA $F_{1,111}=16.26$, $p=0.0001$; riluzole $F_{1,111}=71.98$, $p<0.0001$) (Fig.4.A,B). PMA also targets Munc13-1, leading to augmentation of SV recycling through Munc13-dependent pathway (Betz et al., 1998; Rhee et al., 2002). To occlude PMA-induced activation of Munc13 we used another PKC specific activator, Bryostatin1. As shown in Fig.4.C, this compound increased Syt1-L ab uptake in control cells, but its effect was occluded by co-application of riluzole, supporting the action of riluzole on PKC-dependent pathway (two-way ANOVA; Bryostatin1 $F_{1,73}=30.62$, $p<0.0001$; riluzole $F_{1,73}=96.38$, $p<0.0001$). Moreover, a potent PKC inhibitor, Calpostin-c reduced the efficacy of SV recycling to the similar extent as riluzole alone and there was no additive effects of these compounds (two-way ANOVA; cal-C $F_{1,110}=46.29$, $p<0.0001$; riluzole $F_{1,110}=23.95$, $p<0.0001$) (Fig. 4.D,E). Since Calpostin-c

antagonizes DAG binding and inhibits not only PKC but also Munc13, we also used another PKC inhibitor Ro31-8220. In agreement with cal-C data, both Ro31-8220 and riluzole showed similar effects on Syt11-L ab uptake (two-way ANOVA; Ro31-8220 $F_{1,36}=8.65$, $p=0.0057$; riluzole $F_{1,36}=6.50$, $p=0.0152$) (Fig. 4.F). Altogether, our data suggest that riluzole attenuates SV recycling via inhibition of PKC activity.

PKC has multiple targets within the SV release machinery, including Munc18-1, a member of Sec1/Munc18 family of proteins that are essential for membrane fusion. The PKC-catalyzed phosphorylation of Munc18-1 at Ser313 inhibits the interaction of Munc18-1 with t-SNARE component syntaxin-1 and enables the formation of functional SNARE complex (Fujita et al., 1996) which, in turn, facilitates synaptic activity. Using a p-Ser313 specific antibody we showed that the level of phosphorylated Munc18-1 was significantly upregulated in cells treated with the PKC activator PMA and this effect was completely blocked by the presence of riluzole (two-way ANOVA; PMA $F_{1,43}=1.65$, $p<0.2061$; riluzole $F_{1,43}=5.74$, $p<0.0210$) (Fig.5.A,B). Thus, these experiments identify Munc18-1 as an effector of riluzole-mediated inhibition of PKC signaling. Furthermore, in order to unequivocally prove the involvement of Munc18-1 in riluzole induced lowering of RRP size, we measured the size of RRP in cells where Munc18-1 was downregulated using siRNA approach. The efficacy of Munc18-1 siRNA was confirmed by WB (Fig.5.C) and the size of RRP was assessed by Syt1-L ab uptake assay performed in the presence of 500 mM sucrose. Our data clearly demonstrated the indispensability of Munc18-1 protein in the riluzole mediated regulation of RRP. As shown in Fig.5.D the drug did not have any effect on the RRP size in Munc18-1 depleted cells, whereas we could observe significant downregulation of Syt1-L ab uptake in non-target siRNA (CTRLsiRNA) treated neurons. In line with the previous publication (Toonen et al., 2006) our data revealed that depletion of Munc18-1 also causes a decrease in RRP size in ctrl (vehicle) treated cells (two-way ANOVA; Munc18-1siRNA $F_{1,61}=23.55$, $p<0.0001$; riluzole $F_{1,61}=4.71$, $p<0.0338$)

3.5. Riluzole induced reduction in glutamate levels *in vivo* involves PKC activity

Using an enzyme-based microelectrode array coupled with amperometric recordings (MEA), we monitored the effect of riluzole on cortical glutamate level *in vivo*. MEA technology utilizes high spatial and temporal resolution (<1s) allowing rapid detection of tonic and depolarization (70mM KCl) induced glutamate release and clearance in the brain of living animals (Hascup et al., 2010;

Stan et al., 2014). We recorded evoked glutamate level in prelimbic (PL) and infralimbic (IL) area of the prefrontal cortex in mice upon local application of riluzole (100 μ M) in the presence or absence of PMA. As expected, in both brain areas there was a significant upregulation of the glutamate release in the presence of PKC activator in comparison to vehicle treated animals. However, co-application of PMA and riluzole completely precluded PMA induced glutamate release further confirming that riluzole's antiglutamatergic action is most likely achieved through PKC antagonism and disrupted downstream signaling (two-way ANOVA; PL: PMA $F_{1,26}=9.32$, $p=0.0052$; riluzole $F_{1,26}=15.33$, $p=0.0006$; IL: PMA $F_{1,26}=10.23$, $p=0.0033$; $F_{1,29}=12.54$, $p=0.0014$) (Fig.6.A). Riluzole alone clearly showed a trend towards reduction of glutamate release for about 30%-40%, although not reaching statistical significance in PL and IL cortical areas. However, our data obtained from CA1 region of hippocampus undoubtedly corroborated antiglutamatergic effect of the drug *in vivo* (Fig.5.B; $t(13)=2.667$, $p=0.0194$). Previously, it has been reported that riluzole has a biphasic concentration-dependent effect on basal glutamate uptake by cortical astrocytes (Turck and Frizzo, 2015). The authors showed that at low concentrations (1 and 10 μ M) riluzole significantly increased glutamate uptake, whereas from 100 μ M promoted a slight reduction. In order to test the effect of riluzole on glutamate reuptake *in vivo*, we locally injected 30 μ M of glutamate into mice CA1 region with or without co-application of 100 μ M riluzole. As shown in Fig.6.C there was no difference in decay rate of exogenously applied glutamate (T80) between ctrl and riluzole treated mice ($t(14)=0.7741$, $p=0.4517$).

4. Discussion

Using multifarious live cell imaging techniques, we provide detailed molecular evidence that application of riluzole to primary cortical neurons interferes with the activity of excitatory neurotransmission through the modulation of SV recycling. Live cell imaging coupled with electrical stimulation revealed that the presence of riluzole perturbs the functionality of different SV pools at the presynaptic site. Riluzole-treated cells exhibit smaller RRP, defined as a pool of morphologically docked and fusion competent (“primed”) SVs immediately available for release (Rizzoli and Betz, 2005). Size of RRP is an important factor contributing to all over probability of SV release and its size and the kinetics of release are tightly regulated. Previously it was shown that activation of protein kinase C (PKC) regulates synaptic strength by modulating the size of RRP (Stevens and Sullivan, 1998) and as demonstrated, PKC is inhibited by riluzole (Noh et al., 2000). Our *in vitro* and *in vivo* data convincingly demonstrate that PKC dependent presynaptic potentiation can be completely occluded by co-application of riluzole, providing the functional evidence that riluzole indeed acts as a PKC inhibitor. Alterations in PKC activity and downstream signaling pathways play a significant role in the pathophysiology of mood disorders (Hahn and Friedman, 1999; Zarate and Manji, 2009) and the effect of riluzole on kinase activity might be related to its antidepressant action. In addition, prolonged PKC activation may result in oxidative neuronal injury (Noh et al., 1999) and the effect of riluzole on PKC activity might contribute to its antioxidative and neuroprotective actions. Taken together, riluzole mediated PKC inhibition appears to underlie at least some of its ant glutamatergic effect. PKC has multiple targets within the presynaptic release machinery, including components of the SNARE complex associated with the docking and fusion of vesicles at the site of secretion. Syntaxin binding protein Munc18-1 is essential for neurotransmission and its deletion completely arrests neurotransmitter secretion from synaptic vesicles (Verhage et al., 2000). Also, Munc18-1 is crucial for physiological maintenance of CNS and even subtle alterations in Munc18-1 have been shown to cause severe neuropsychiatric disorders with cognitive impairments (Ramos-Miguel et al., 2015). Interestingly, Munc18-1 has been identified as a PKC substrate (Barclay et al., 2003). Phosphorylation of Munc18-1 by PKC at Ser313 inhibits the interaction of Munc18-1 with syntaxin-1 (de Vries et al., 2000) and enables the formation of the functional SNARE complex

which impacts SV recycling. Here we showed that riluzole completely blocked the induction of Munc18-1 phosphorylation by the PKC activator, PMA, in primary cortical cells, suggesting that Munc18-1 may be a downstream target of the drug whose phosphorylation status determines the rate of glutamate release. Furthermore, by using the siRNA approach we also showed that the effect of riluzole on RRP is completely precluded upon Munc18-1 depletion from the cells.

By monitoring the uptake of flourophore coupled syt1-L ab we showed that both resting and activity induced SV release was markedly attenuated in riluzole treated cells. Sensitivity of affected synapses to riluzole was reversible and their activity returned to baseline after washout. Previously it has been reported that riluzole selectively blocks glutamate over GABA release (Prakriya and Mennerick, 2000), and here we confirm that network activity driven syt1-L ab uptake upon riluzole application was affected only in synapses positive for the excitatory marker VGLUT1. Furthermore, we also showed that following riluzole treatment VGLUT1 immunoreactivity was prominently decreased, suggesting lower vesicular loading capacity and consequently lower quantal size of glutamate release. These data corroborate previous findings that riluzole, similiary to the anticonvulsant drug valproate, saliently reduced VGLUT1 immunoreactivity in epilepsy animal models (Kim et al., 2007a). Reduction of VGLUT1 immunoreactivity was linked to the elevation of the seizure threshold and the function of riluzole as an antiepileptic drug. Interestingly, in our model system, riluzole did not influence the activity of inhibitory synapses but impelled synaptic accumulation of VGAT, implying increased GABA load into SV. This result together with previously published data that riluzole blocks GABA uptake and promotes accumulation of GABA within the synaptic cleft (Mantz et al., 1994) suggests a change of E/I transmission upon riluzole treatment that may also contribute to its anticonvulsant properties.

Efficient neurotransmission requires structural and functional integrity of SVs and presynaptic compartment. As shown, riluzole-treated cells exhibit severe depletion of integral SV and SNARE proteins within individual synapses, which together with rearrangement of other presynaptic scaffolds, could account for lower SV recycling. Munc13-1 is the other molecule, beside Munc18-1, involved in SNARE complex assembly and regulation of SV recycling (Lai et al., 2017). Recent studies showed that Munc18-1 and Munc13-1 together stabilize release-ready vesicles by preventing de-priming (Lai et al., 2017; Ma et al., 2011). Therefore, reduced synaptic

level of Munc13-1 in riluzole treated cells may also contribute to the reduction of RRP. Reduced presynaptic activity in the presence of riluzole alters postsynaptic glutamate sensitivity, and in order to maintain relatively homeostatic response, riluzole treated neurons compensate for changes in excitatory synaptic input through accumulation of GluA1 receptors at the postsynaptic membrane. Activity dependent accumulation of postsynaptic AMPA receptors is a well-known phenomenon, described by O'Brien et al (O'Brien et al., 1998) as a regulatory process that plays a critical role in the modulation of both normal and pathological neuronal functions. It is still unknown whether there is a similar effect of riluzole on surface NMDA receptors, but an electrophysiological study from Rammes et al. (2008) showed that the fraction of activated NMDA receptors during synaptic transmission remains constant in the presence of the glutamate release inhibitor riluzole.

Taken together, our study unravels molecular mechanisms underlying antiglutamatergic properties of riluzole which might account for its antidepressant and neuroprotective activities. In particular, we report novel data suggesting that riluzole attenuates excitatory neurotransmission by interfering with SV recycling and reducing the size of RRP through PKC/Munc18-1 and Munc13-1 dependent mechanisms.

Acknowledgements:

We thank Charbel Antoine Kreidy and Ioannis Madas for the technical assistance, Noam Ziv for providing the OpenView software and Mikael Svensson for maintenance of the ZEISS LSM 880 Airyscan microscope. We also thank Holly Green and Jean-Ha Baek for proofreading.

Funding and Disclosure

This work has been financially supported by the Swedish Research Council and a STINT sponsored collaboration with China. The authors declare no conflict of interest.

References:

Alabi, A. A., Tsien, R. W., 2012. Synaptic vesicle pools and dynamics. *Cold Spring Harb Perspect Biol* 4, a013680.

- Alvarsson, A., Zhang, X., Stan, T. L., Schintu, N., Kadkhodaei, B., Millan, M. J., Perlmann, T., Svenningsson, P., 2015. Modulation by Trace Amine-Associated Receptor 1 of Experimental Parkinsonism, L-DOPA Responsivity, and Glutamatergic Neurotransmission. *J Neurosci* 35, 14057-14069.
- Andreae, L. C., Fredj, N. B., Burrone, J., 2012. Independent vesicle pools underlie different modes of release during neuronal development. *J Neurosci* 32, 1867-1874.
- Barclay, J. W., Craig, T. J., Fisher, R. J., Ciuffo, L. F., Evans, G. J., Morgan, A., Burgoyne, R. D., 2003. Phosphorylation of Munc18 by protein kinase C regulates the kinetics of exocytosis. *J Biol Chem* 278, 10538-10545.
- Betz, A., Ashery, U., Rickmann, M., Augustin, I., Neher, E., Sudhof, T. C., Rettig, J., Brose, N., 1998. Munc13-1 is a presynaptic phorbol ester receptor that enhances neurotransmitter release. *Neuron* 21, 123-136.
- Borowicz, K. K., Sekowski, A., Drelewska, E., Czuczwar, S. J., 2004. Riluzole enhances the anti-seizure action of conventional antiepileptic drugs against pentetrazole-induced convulsions in mice. *Pol J Pharmacol* 56, 187-193.
- Bruijn, L. I., Miller, T. M., Cleveland, D. W., 2004. Unraveling the mechanisms involved in motor neuron degeneration in ALS. *Annu Rev Neurosci* 27, 723-749.
- Centonze, D., Calabresi, P., Pisani, A., Marinelli, S., Marfia, G. A., Bernardi, G., 1998. Electrophysiology of the neuroprotective agent riluzole on striatal spiny neurons. *Neuropharmacology* 37, 1063-1070.
- de Vries, K. J., Geijtenbeek, A., Brian, E. C., de Graan, P. N., Ghijsen, W. E., Verhage, M., 2000. Dynamics of munc18-1 phosphorylation/dephosphorylation in rat brain nerve terminals. *Eur J Neurosci* 12, 385-390.
- Du, J., Suzuki, K., Wei, Y., Wang, Y., Blumenthal, R., Chen, Z., Falke, C., Zarate, C. A., Jr., Manji, H. K., 2007. The anticonvulsants lamotrigine, riluzole, and valproate differentially regulate AMPA receptor membrane localization: relationship to clinical effects in mood disorders. *Neuropsychopharmacology* 32, 793-802.
- Duman, R. S., Aghajanian, G. K., 2012. Synaptic dysfunction in depression: potential therapeutic targets. *Science* 338, 68-72.
- Frizzo, M. E., Dall'Onder, L. P., Dalcin, K. B., Souza, D. O., 2004. Riluzole enhances glutamate uptake in rat astrocyte cultures. *Cell Mol Neurobiol* 24, 123-128.
- Fujita, Y., Sasaki, T., Fukui, K., Kotani, H., Kimura, T., Hata, Y., Sudhof, T. C., Scheller, R. H., Takai, Y., 1996. Phosphorylation of Munc-18/n-Sec1/rbSec1 by protein kinase C: its implication in regulating the interaction of Munc-18/n-Sec1/rbSec1 with syntaxin. *J Biol Chem* 271, 7265-7268.
- Fumagalli, E., Funicello, M., Rauen, T., Gobbi, M., Mennini, T., 2008. Riluzole enhances the activity of glutamate transporters GLAST, GLT1 and EAAC1. *Eur J Pharmacol* 578, 171-176.
- Grant, P., Song, J. Y., Swedo, S. E., 2010. Review of the use of the glutamate antagonist riluzole in psychiatric disorders and a description of recent use in childhood obsessive-compulsive disorder. *J Child Adolesc Psychopharmacol* 20, 309-315.
- Gundelfinger, E. D., Fejtova, A., 2012. Molecular organization and plasticity of the cytomatrix at the active zone. *Curr Opin Neurobiol* 22, 423-430.
- Hahn, C. G., Friedman, E., 1999. Abnormalities in protein kinase C signaling and the pathophysiology of bipolar disorder. *Bipolar Disord* 1, 81-86.
- Hascup, E. R., Hascup, K. N., Stephens, M., Pomerleau, F., Huettl, P., Gratton, A., Gerhardt, G. A., 2010. Rapid microelectrode measurements and the origin and regulation of extracellular glutamate in rat prefrontal cortex. *J Neurochem* 115, 1608-1620.
- Hua, Y., Sinha, R., Thiel, C. S., Schmidt, R., Huve, J., Martens, H., Hell, S. W., Egner, A., Klingauf, J., 2011. A readily retrievable pool of synaptic vesicles. *Nat Neurosci* 14, 833-839.

- Hunsberger, H. C., Weitzner, D. S., Rudy, C. C., Hickman, J. E., Libell, E. M., Speer, R. R., Gerhardt, G. A., Reed, M. N., 2015. Riluzole rescues glutamate alterations, cognitive deficits, and tau pathology associated with P301L tau expression. *J Neurochem* 135, 381-394.
- Kim, J. E., Kim, D. S., Kwak, S. E., Choi, H. C., Song, H. K., Choi, S. Y., Kwon, O. S., Kim, Y. I., Kang, T. C., 2007a. Anti-glutamatergic effect of riluzole: comparison with valproic acid. *Neuroscience* 147, 136-145.
- Kim, M. J., Futai, K., Jo, J., Hayashi, Y., Cho, K., Sheng, M., 2007b. Synaptic accumulation of PSD-95 and synaptic function regulated by phosphorylation of serine-295 of PSD-95. *Neuron* 56, 488-502.
- Lai, Y., Choi, U. B., Leitz, J., Rhee, H. J., Lee, C., Altas, B., Zhao, M., Pfuetzner, R. A., Wang, A. L., Brose, N., Rhee, J., Brunger, A. T., 2017. Molecular Mechanisms of Synaptic Vesicle Priming by Munc13 and Munc18. *Neuron* 95, 591-607 e510.
- Lazarevic, V., Schone, C., Heine, M., Gundelfinger, E. D., Fejtova, A., 2011. Extensive remodeling of the presynaptic cytomatrix upon homeostatic adaptation to network activity silencing. *J Neurosci* 31, 10189-10200.
- Lener, M. S., Kadriu, B., Zarate, C. A., Jr., 2017. Ketamine and Beyond: Investigations into the Potential of Glutamatergic Agents to Treat Depression. *Drugs*.
- Ma, C., Li, W., Xu, Y., Rizo, J., 2011. Munc13 mediates the transition from the closed syntaxin-Munc18 complex to the SNARE complex. *Nat Struct Mol Biol* 18, 542-549.
- Mantz, J., Laudenbach, V., Lecharny, J. B., Henzel, D., Desmonts, J. M., 1994. Riluzole, a novel antigitamate, blocks GABA uptake by striatal synaptosomes. *Eur J Pharmacol* 257, R7-8.
- Mathew, S. J., Gueorguieva, R., Brandt, C., Fava, M., Sanacora, G., 2017. A Randomized, Double-Blind, Placebo-Controlled, Sequential Parallel Comparison Design Trial of Adjunctive Riluzole for Treatment-Resistant Major Depressive Disorder. *Neuropsychopharmacology* 42, 2567-2574.
- Noh, K. M., Hwang, J. Y., Shin, H. C., Koh, J. Y., 2000. A novel neuroprotective mechanism of riluzole: direct inhibition of protein kinase C. *Neurobiol Dis* 7, 375-383.
- Noh, K. M., Kim, Y. H., Koh, J. Y., 1999. Mediation by membrane protein kinase C of zinc-induced oxidative neuronal injury in mouse cortical cultures. *J Neurochem* 72, 1609-1616.
- O'Brien, R. J., Kamboj, S., Ehlers, M. D., Rosen, K. R., Fischbach, G. D., Huganir, R. L., 1998. Activity-dependent modulation of synaptic AMPA receptor accumulation. *Neuron* 21, 1067-1078.
- Park, L. T., Lener, M. S., Hopkins, M., Iadorola, N., Machado-Vieira, R., Ballard, E., Nugent, A., Zarate, C. A., Jr., 2017. A Double-Blind, Placebo-Controlled, Pilot Study of Riluzole Monotherapy for Acute Bipolar Depression. *J Clin Psychopharmacol* 37, 355-358.
- Pereira, A. C., Lambert, H. K., Grossman, Y. S., Dumitriu, D., Waldman, R., Jannetty, S. K., Calakos, K., Janssen, W. G., McEwen, B. S., Morrison, J. H., 2014. Glutamatergic regulation prevents hippocampal-dependent age-related cognitive decline through dendritic spine clustering. *Proc Natl Acad Sci U S A* 111, 18733-18738.
- Prakriya, M., Mennerick, S., 2000. Selective depression of low-release probability excitatory synapses by sodium channel blockers. *Neuron* 26, 671-682.
- Rammes, G., Zieglgansberger, W., Parsons, C. G., 2008. The fraction of activated N-methyl-D-aspartate receptors during synaptic transmission remains constant in the presence of the glutamate release inhibitor riluzole. *J Neural Transm (Vienna)* 115, 1119-1126.
- Ramos-Miguel, A., Hercher, C., Beasley, C. L., Barr, A. M., Bayer, T. A., Falkai, P., Leurgans, S. E., Schneider, J. A., Bennett, D. A., Honer, W. G., 2015. Loss of Munc18-1 long splice variant in GABAergic terminals is associated with cognitive decline and increased risk of dementia in a community sample. *Mol Neurodegener* 10, 65.
- Rhee, J. S., Betz, A., Pyott, S., Reim, K., Varoqueaux, F., Augustin, I., Hesse, D., Sudhof, T. C., Takahashi, M., Rosenmund, C., Brose, N., 2002. Beta phorbol ester- and diacylglycerol-induced augmentation of transmitter release is mediated by Munc13s and not by PKCs. *Cell* 108, 121-133.
- Rizzoli, S. O., Betz, W. J., 2005. Synaptic vesicle pools. *Nat Rev Neurosci* 6, 57-69.

- Romano, S., Coarelli, G., Marcotulli, C., Leonardi, L., Piccolo, F., Spadaro, M., Frontali, M., Ferraldeschi, M., Vulpiani, M. C., Ponzelli, F., Salvetti, M., Orzi, F., Petrucci, A., Vanacore, N., Casali, C., Ristori, G., 2015. Riluzole in patients with hereditary cerebellar ataxia: a randomised, double-blind, placebo-controlled trial. *Lancet Neurol* 14, 985-991.
- Rosenmund, C., Stevens, C. F., 1996. Definition of the readily releasable pool of vesicles at hippocampal synapses. *Neuron* 16, 1197-1207.
- Salardini, E., Zeinoddini, A., Mohammadinejad, P., Khodaie-Ardakani, M. R., Zahraei, N., Zeinoddini, A., Akhondzadeh, S., 2016. Riluzole combination therapy for moderate-to-severe major depressive disorder: A randomized, double-blind, placebo-controlled trial. *J Psychiatr Res* 75, 24-30.
- Sanacora, G., Kendell, S. F., Levin, Y., Simen, A. A., Fenton, L. R., Coric, V., Krystal, J. H., 2007. Preliminary evidence of riluzole efficacy in antidepressant-treated patients with residual depressive symptoms. *Biol Psychiatry* 61, 822-825.
- Sanacora, G., Treccani, G., Popoli, M., 2012. Towards a glutamate hypothesis of depression: an emerging frontier of neuropsychopharmacology for mood disorders. *Neuropharmacology* 62, 63-77.
- Stan, T. L., Alvarsson, A., Branzell, N., Sousa, V. C., Svenningsson, P., 2014. NMDA receptor antagonists ketamine and Ro25-6981 inhibit evoked release of glutamate in vivo in the subiculum. *Transl Psychiatry* 4, e395.
- Stevens, C. F., Sullivan, J. M., 1998. Regulation of the readily releasable vesicle pool by protein kinase C. *Neuron* 21, 885-893.
- Toonen, R. F., Wierda, K., Sons, M. S., de Wit, H., Cornelisse, L. N., Brussaard, A., Plomp, J. J., Verhage, M., 2006. Munc18-1 expression levels control synapse recovery by regulating readily releasable pool size. *Proc Natl Acad Sci U S A* 103, 18332-18337.
- Tsuriel, S., Geva, R., Zamorano, P., Dresbach, T., Boeckers, T., Gundelfinger, E. D., Garner, C. C., Ziv, N. E., 2006. Local sharing as a predominant determinant of synaptic matrix molecular dynamics. *PLoS Biol* 4, e271.
- Turck, P., Frizzo, M. E., 2015. Riluzole stimulates BDNF release from human platelets. *Biomed Res Int* 2015, 189307.
- Umemiya, M., Berger, A. J., 1995. Inhibition by riluzole of glycinergic postsynaptic currents in rat hypoglossal motoneurons. *Br J Pharmacol* 116, 3227-3230.
- Urbani, A., Belluzzi, O., 2000. Riluzole inhibits the persistent sodium current in mammalian CNS neurons. *Eur J Neurosci* 12, 3567-3574.
- Wang, S. J., Wang, K. Y., Wang, W. C., 2004. Mechanisms underlying the riluzole inhibition of glutamate release from rat cerebral cortex nerve terminals (synaptosomes). *Neuroscience* 125, 191-201.
- Verhage, M., Maia, A. S., Plomp, J. J., Brussaard, A. B., Heeroma, J. H., Vermeer, H., Toonen, R. F., Hammer, R. E., van den Berg, T. K., Missler, M., Geuze, H. J., Sudhof, T. C., 2000. Synaptic assembly of the brain in the absence of neurotransmitter secretion. *Science* 287, 864-869.
- Zarate, C. A., Manji, H. K., 2009. Protein kinase C inhibitors: rationale for use and potential in the treatment of bipolar disorder. *CNS Drugs* 23, 569-582.
- Zona, C., Cavalcanti, S., De Sarro, G., Siniscalchi, A., Marchetti, C., Gaetti, C., Costa, N., Mercuri, N., Bernardi, G., 2002. Kainate-induced currents in rat cortical neurons in culture are modulated by riluzole. *Synapse* 43, 244-251.

Figure legends

Fig.1. Riluzole attenuates the activity of glutamatergic synapses. **A)** Representative images of primary cortical neurons treated with 100 μ M riluzole or control solution for 90 min and stained with syt1-L ab and sph (green in overlay picture) immediately or 24h after riluzole/control solution washout. **B)** Quantification of network activity driven syt-1L ab uptake along 20 μ m of proximal dendrite in given conditions. **(C)** Representative images of syt-1L ab and sph (green in overlay picture) staining in three weeks old primary cortical cells exposed to control solution, riluzole or 48h of activity deprivation (D-AP5/CNQX) with or without riluzole treatment. **D)** Corresponding quantification of syt1-L ab uptake along 20 μ m of proximal dendrite driven by spontaneous network activity. **E)** Representative images and quantification **(F)** of syt-1L ab uptake in VGLUT1 (green in overlays) and VGAT (green in overlays) positive puncta in control or cells exposed to 100 μ M riluzole for 90 min. **G)** VGLUT1 and VGAT immunoreactivity quantification in control and riluzole treated cells along 20 μ m of proximal dendrite. In all graphs, bars denote intensity values normalized to the mean intensity value in the control group \pm SEM. The statistic was assessed using two-way ANOVA followed by Bonferroni's multiple comparison test (B,D) and Student's t-test (F, G). * p <0.05, ** p <0.01, *** p <0.001 **** p <0.0001. Scale bar, 5 μ m.

Abbreviations: syt1-L ab (synaptotagmin 1 luminal domain antibody); sph (synaptophysin); VGLUT1 (Vesicular Glutamate Transporter 1); VGAT (Vesicular GABA Transporter)

Fig.2. Riluzole decreases the size of RRP. **A)** Average syt1-cypHer fluorescence traces and quantifications reporting SV pool sizes from control and Riluzole treated neurons. The neurons were imaged in the presence of the proton pump inhibitor bafilomycin A (1 μ M). The vesicles from the RRP were released by stimulation with 40AP at 20Hz. This was followed by a 2 min period without stimulation and a train of 200AP at 20Hz which triggered the release of the vesicles from the RP. The fluorescence responses representing the sizes of the RRP and the RP are given as fractions of the total Syt1-L-CypHer labeling. **B)** Staining of control and riluzole (100 μ M, 90min) treated cells with syt1-L ab and sph (green in overlay picture) upon exposure to 500 mM sucrose for 4 min. **C)** quantification of sucrose evoked syt1-L ab uptake along 20 μ m of proximal dendrite in control and riluzole treated cells. Statistic was done using Student's t-test ** $p < 0.01$, **** $p < 0.0001$. Scale bar, 5 μ m.

Fig.3. Riluzole induces subtle remodeling of pre- and postsynaptic compartments. **A)** Representative images of CTRL and riluzole treated cells stained for indicated synaptic proteins and **B)** quantification of the immunofluorescence signal along 20 μ m of proximal dendrite. **C)** Sample of western blot showing total and surface expression of GluA1 in control and riluzole treated cells. **D)** Representative images of control and riluzole treated cortical neurons stained for surface GluA and sph (green in overlays) and **(E)** corresponding quantification of GluA surface expression. **F)** Staining of postsynaptic proteins PSD95 and Homer1 in primary cortical neurons after exposure to control solution or riluzole with quantification **(G)** of the immunofluorescence signal along 20 μ m of proximal dendrite. Bars in (B), (E) and (G) represent data normalized to the mean of the control group and expressed as mean \pm SEM. Statistical significance was assessed using Student's t-test. * $p < 0.05$, ** $p < 0.01$, *** $p < 0.001$ **** $p < 0.0001$. Scale bar, 5 μ m.

Fig.4. Riluzole attenuates SV recycling by interfering with PKC activity. **A)** Representative images and quantification of Syt1-L ab uptake assay in primary cortical neurons treated with **(B)** control solution, PKC activator (200 nM PMA, 20 min pretreatment), PMA/riluzole or riluzole alone (100 μ M, 90 min) or **(C)** Bryostatin 1 (0.27nM, 30 min pretreatment) in the presence or absence of riluzole. **D)** Exemplary images of cells stained with Syt1-L ab upon treatment with control solution, PKC inhibitor (cal-C, 20 min pre-treatment, 1 μ M), cal-C/riluzole or riluzole

alone (100 μ M, 90 min). **E)** Quantification of **D**. **F)** Quantification of Syt1-L ab uptake in cells treated with control solution, PKC inhibitor (Ro 31-8220, 20 min pre-treatment, 3.3 μ M), Ro 31-8220/riluzole or riluzole alone (100 μ M, 90 min). Statistical significance was evaluated using two-way ANOVA followed by Bonferroni multiple comparison test. *** $p < 0.01$, **** $p < 0.0001$. Scale bar, 5 μ m.

Fig.5. Involvement of Munc18-1 in riluzole induced lowering of RRP size. **A)** Western blot of neuronal extracts from primary cortical neurons treated with PMA or control solution in the presence or absence of riluzole, using antibodies specific for pMunc18-1 (S313) and total Munc18-1. **B)** Statistical assessment of pMunc18-1 (Ser313) signal in given conditions. Results are representative of 4 independent experiments. Signal of pMunc18-1 (Ser313) was normalized to its total expression level for each condition and expressed as % of the signal in CTRL cells. **C)** Representative western blot showing the efficiency of Munc18-1 knockdown using Munc18-1 siRNA or non-targeting (CTRL) siRNA. **D)** Quantification of sucrose evoked syt1-L ab uptake along 20 μ m of proximal dendrite in control and riluzole treated cells with and without Munc18-1 depletion. Statistical significance was evaluated using two-way ANOVA followed by Bonferroni multiple comparison test. ** $p < 0.01$, *** $p < 0.01$, **** $p < 0.0001$.

Fig.6. Effects of acute riluzole and PMA application on KCl evoked glutamate release in prelimbic and infralimbic area of the cortex. **A)** Evoked glutamate amplitude (in the presence of 70mM KCl) was significantly increased in both PL and IF cortex of mice upon local PMA injection and this effect was completely blocked by co-application of riluzole. An insert shows the traces of glutamate responses in given conditions. **B)** Quantification of the glutamate release from CA1 region of hippocampus upon local application of riluzole. **C)** Decay rate of exogenously applied glutamate in the CA1 in the presence and absence of riluzole. Graphs represent the mean \pm SEM. * $p < 0.05$, ** $p < 0.01$, *** $p < 0.001$ by two-way ANOVA and Bonferroni multiple comparison test (A) and Student's t-test (B).

*Supplementary figures***S1) Riluzole reduces presynaptic activity in a concentration-dependent manner.**

Quantification of network activity driven syt-1L ab uptake along 20 μ m of proximal dendrite upon 90 min exposure to different concentrations of riluzole. Statistical significance was assessed using one-way ANOVA and Bonferroni multiple comparison test, **p<0.01, ***p<0.001

S2) Riluzole induced reduction of presynaptic proteins at the level of individual synapses is not due to increased proteasomal degradation.

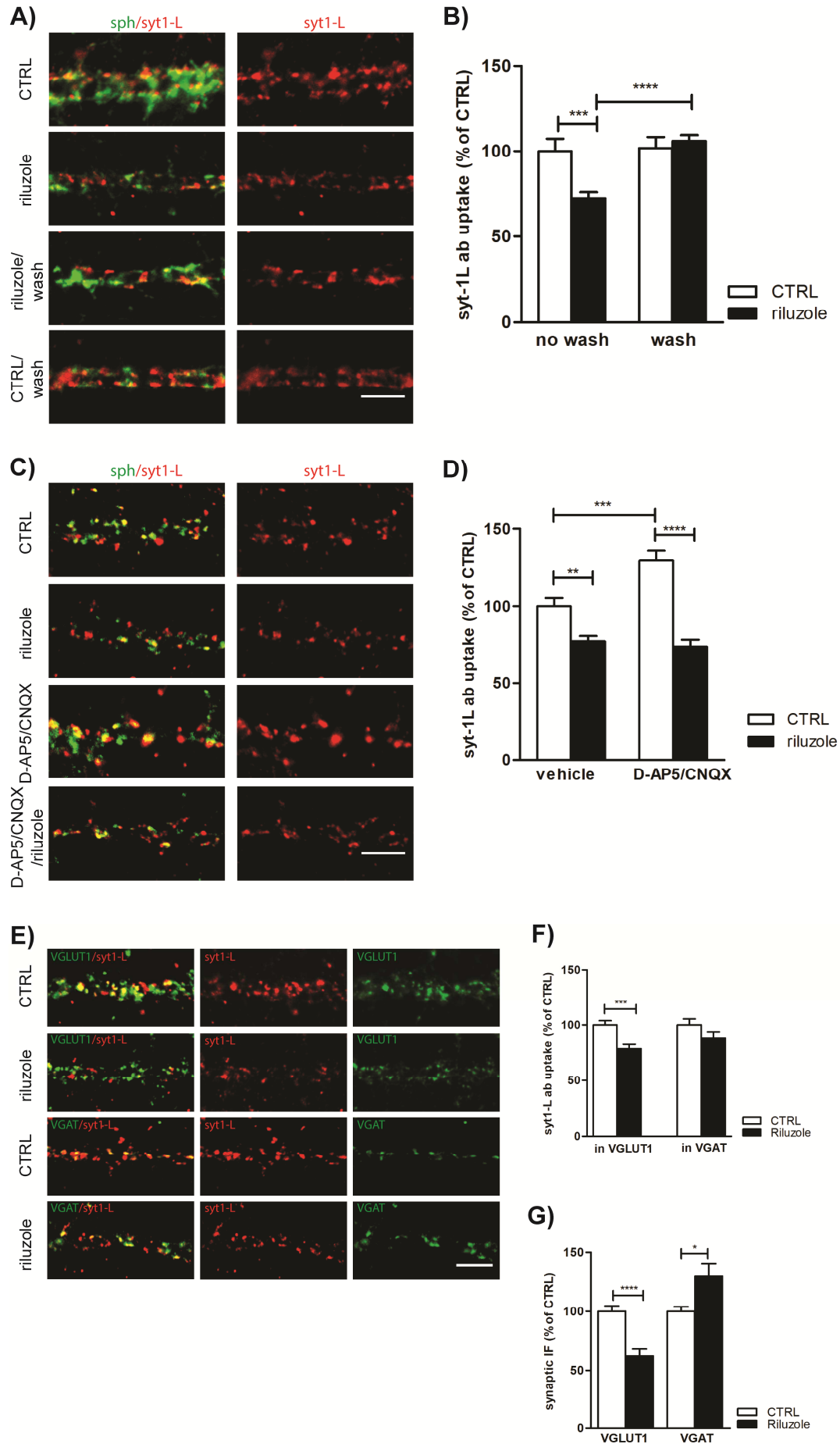
Quantification of the immunofluorescence signal along 20 μ m of proximal dendrites in cells pretreated with proteasome inhibitor MG132 30 min before treatment with riluzole or vehicle. Bars represent fluorescence normalized to the mean intensity value of MG132 treated cells and expressed as % \pm SEM. Statistical significance was assessed using Student's t-test, **p<0.01, ***p<0.001, ****p<0.0001

S3) Riluzole does not influence the total level of proteins involved in neurotransmission.

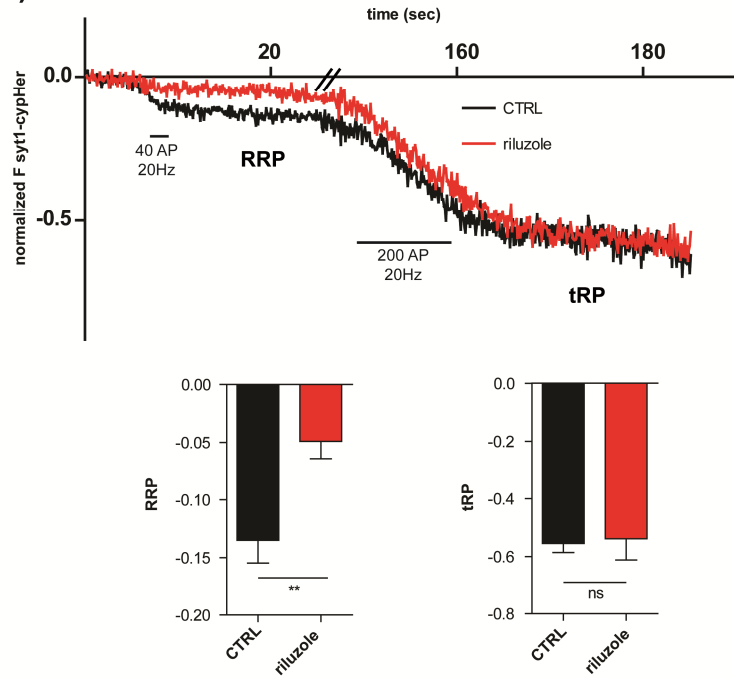
Quantification of the signal from selected pre-and postsynaptic proteins isolated from three weeks old cortical neurons treated for 90 min with control solution or 100 μ M riluzole. The intensity of the signal for each protein was normalized to β -Tubulin and expressed as % of

control. Data are from 3 independent experiments. Statistical significance was evaluated by using Student's t-test.

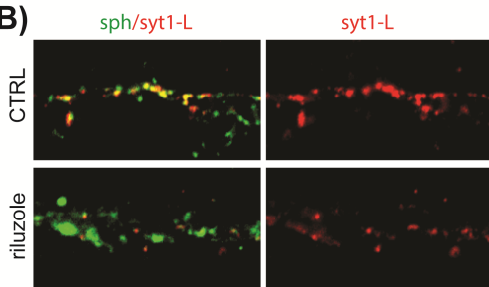
ACCEPTED MANUSCRIPT



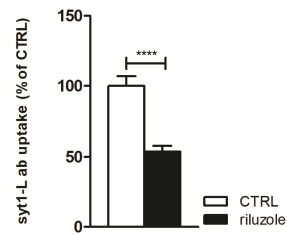
A)

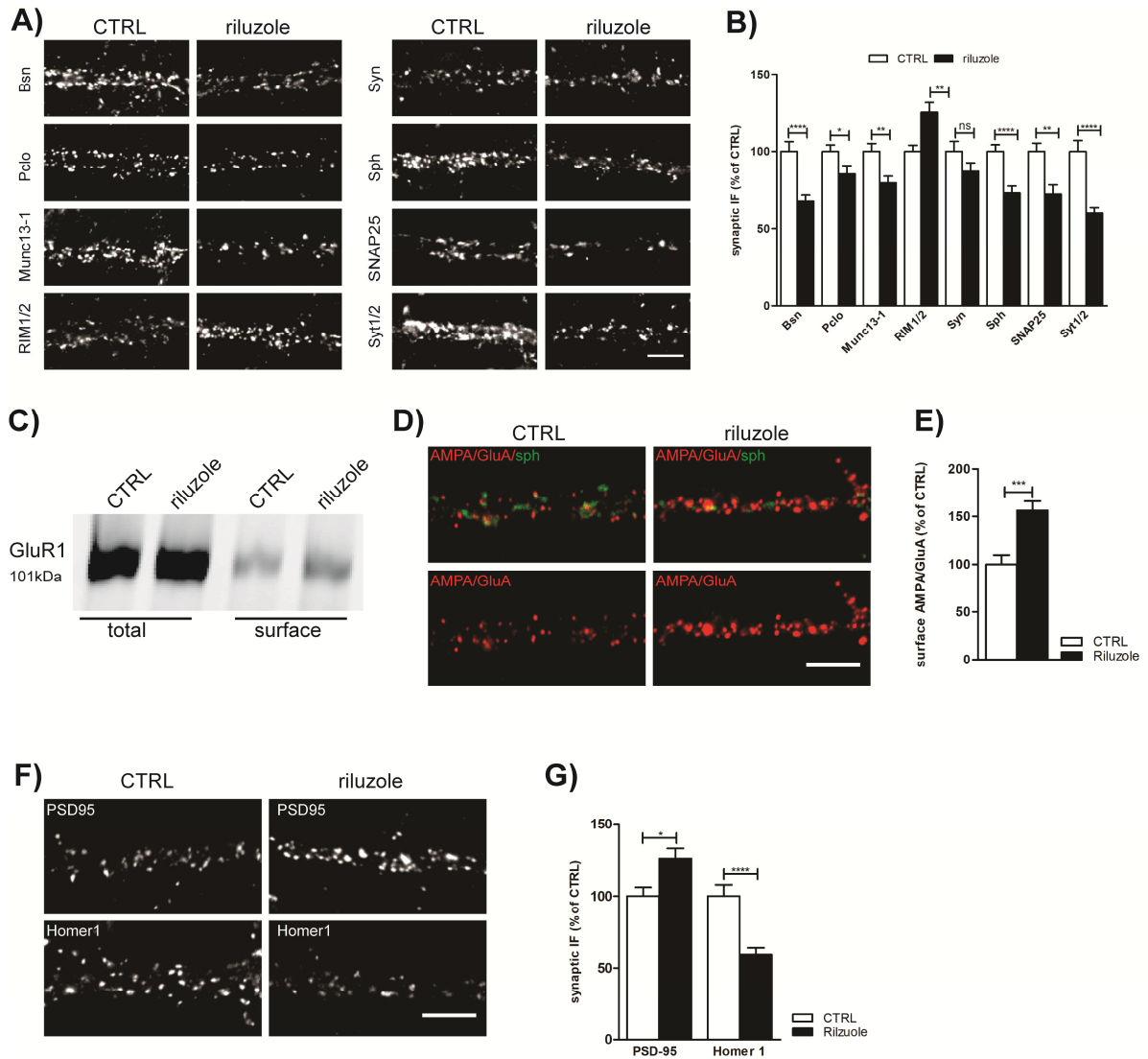


B)

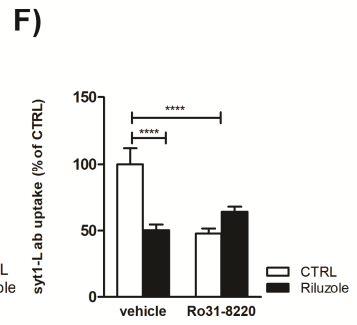
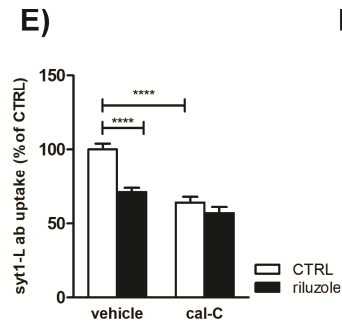
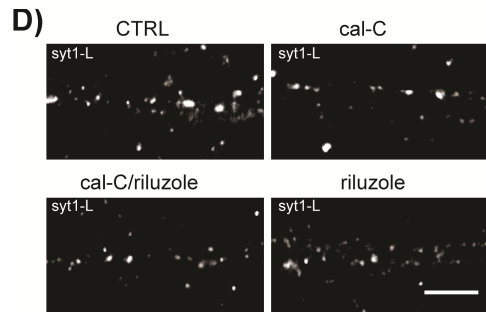
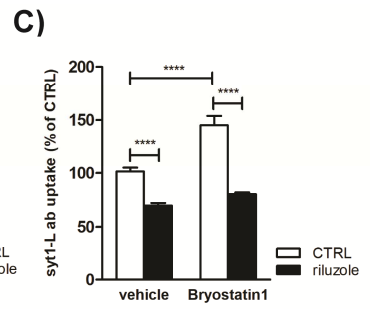
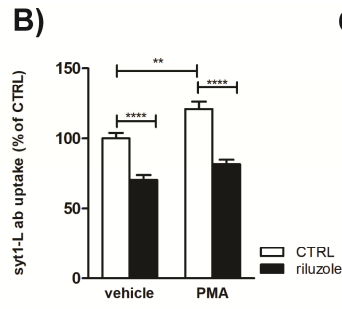
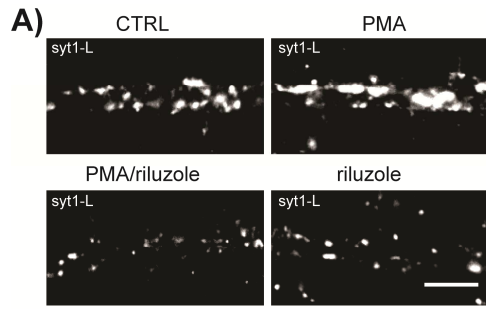


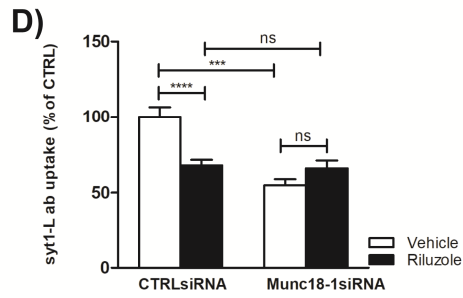
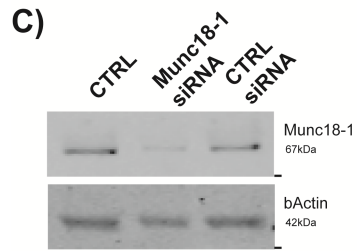
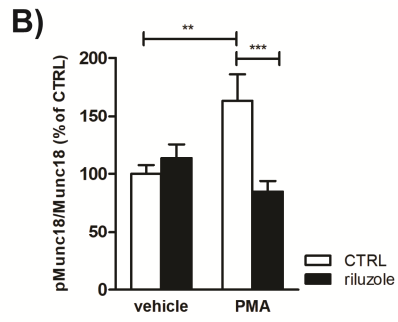
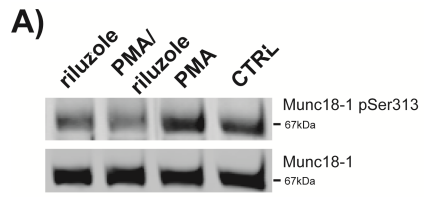
C)



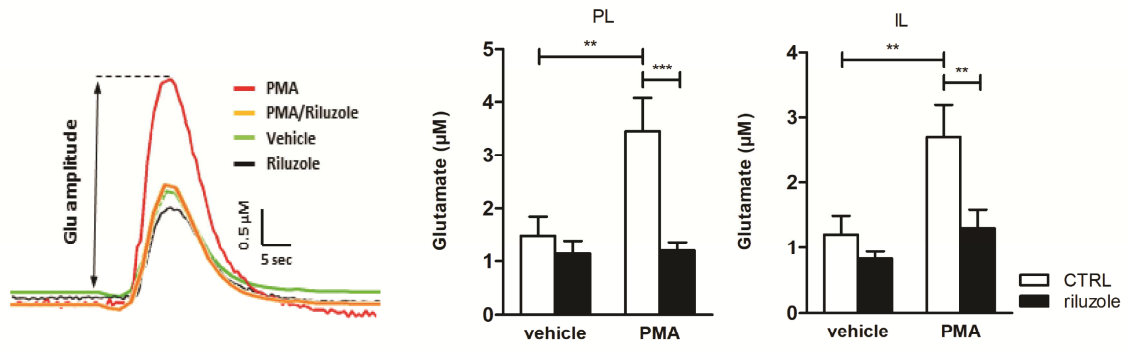


ACCEPTED MANUSCRIPT

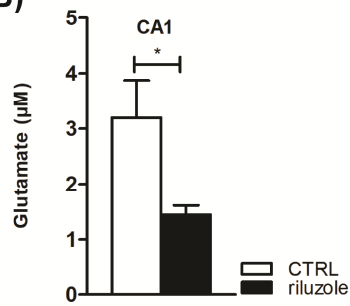




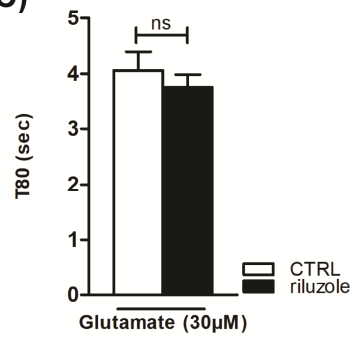
A)



B)



C)



Highlights

- riluzole attenuates excitatory neurotransmission by interfering with SV recycling
- riluzole induces molecular remodeling of pre-and postsynaptic compartment
- Munc18 is an effector of riluzole-mediated inhibition of PKC signaling